

Measurement of the Lamb Shift in Lithiumlike Uranium (U^{89+})

J. Schweppe,^{(1),(a)} A. Belkacem,^{(1),(b)} L. Blumenfeld,^{(1),(c)} Nelson Claytor,^{(1),(d)} B. Feinberg,^{(2),(e)} Harvey Gould,^{(1),(f)} V. E. Kostroun,^{(1),(g)} L. Levy,^{(2),(h)} S. Misawa,^{(1),(g)} J. R. Mowat,^{(1),(i)} and M. H. Prior^{(1),(j)}

⁽¹⁾*Chemical Sciences Division, Building 71-259, Lawrence Berkeley Laboratory,
One Cyclotron Road, Berkeley, California 94720*

⁽²⁾*Accelerator and Fusion Research Division, Building 51-208, Lawrence Berkeley Laboratory,
One Cyclotron Road, Berkeley, California 94720*

(Received 10 December 1990)

The $2^2P_{1/2}$ - $2^2S_{1/2}$ (lowest-excited-state to ground-state) energy splitting in lithiumlike uranium, which has large quantum-electrodynamic corrections, has been measured using Doppler-tuned spectrometry. Our result, 280.59 ± 0.10 eV, is more precise than current theory and is an 80-fold improvement over the previous most precise measurement of the Lamb shift in (heliumlike) uranium.

PACS numbers: 31.30.Jv, 12.20.Fv, 32.70.Fw

In few-electron, high-nuclear-charge (Z) ions, the largest quantum-electrodynamic (QED) contribution to the binding energy comes from terms in the electron self-energy which are high powers¹ of $Z\alpha$ and thus can only be tested in very-high- Z experiments. The $2^2P_{1/2}$ - $2^2S_{1/2}$ splitting in a hydrogenlike atom (the one-electron Lamb shift) also contains a contribution from the vacuum polarization, which is well tested in muonic atom experiments,² and non-QED contributions from finite nuclear size and nuclear polarizability. The calculation of the above terms is sufficient for a comparison of Lamb-shift theory and experiment in hydrogenlike uranium.

Our experiment uses lithiumlike uranium because its long-lived $2^2P_{1/2}$ state (62 ps) allows us to measure the $1s^22p^22^2P_{1/2}$ - $1s^22s^22^2S_{1/2}$ (lowest-excited-state to ground-state) transition energy in vacuum, far downstream from the target in which the $2^2P_{1/2}$ state is formed. (The decay of the $1s2p^23P_0$ state of heliumlike uranium which has a lifetime of ≈ 54 ps can also be observed in vacuum.) This avoids any perturbation of the transition energy due to the target atoms—not possible in hydrogenlike uranium, whose $n=2$ levels decay in less than 10^{-14} s.

To test QED in few-electron uranium, theory must also account for the relativistic Coulomb interaction between electrons, the screening of the self-energy, and vacuum polarization. The theoretical uncertainty in these contributions is currently of the order of 1 eV. Thus, for the present, our experiment is far more precise than theory.

Previously, the most precise determination of the Lamb shift in uranium³ (with an experimental uncertainty of 7.9 eV) used a measurement of the heliumlike $1s2p^23P_0$ lifetime to infer the $1s2p^23P_0$ - $1s2s^23S_1$ transition energy, and, in turn, the one-electron Lamb shift. In this Letter we report an improvement in the experimental precision to 0.1 eV by a direct measurement of the corresponding transition energy in lithiumlike uranium.

Lithiumlike uranium (U^{89+}) is produced by stripping a beam of ≈ 95 MeV/u U^{40+} ($\beta = v/c \approx 0.42$), obtained from the Lawrence Berkeley Laboratory's Bevalac heavy-ion accelerator, in a 2000-mg/cm² aluminum foil and magnetically selecting the ($\approx 30\%$) U^{89+} fraction. The U^{89+} is transported about 50 m to the experiment, where a 1.69-mg/cm² aluminum target foil collisionally excites approximately 18% of the ions, initially in their ground state, into the $2^2P_{1/2}$ state, which then decays downstream with a decay length of about 0.8 cm.

We measure the 281-eV $2^2P_{1/2}$ - $2^2S_{1/2}$ lithiumlike uranium transition energy using a Doppler-tuned spectrometer⁴ (Fig. 1). Because the photons with energy ω_{ion} are emitted from a moving source, their energy is seen Doppler shifted in the laboratory to energy ω_{lab} :

$$\omega_{ion} = \omega_{lab}(1 - \beta \cos\theta_{lab}) / (1 - \beta^2)^{1/2}, \quad (1)$$

where θ_{lab} is the viewing angle in the laboratory measured from the beam direction. When viewed through a column of argon gas, the photons are absorbed as the

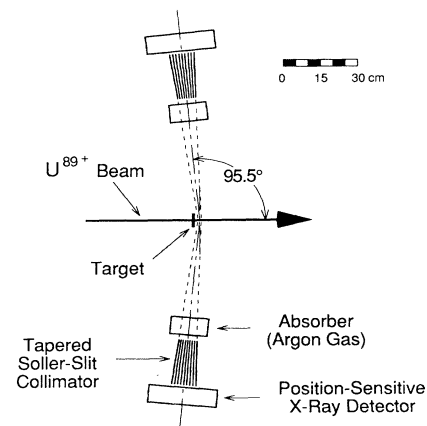


FIG. 1. A schematic diagram of the Doppler-tuned spectrometer. Two of the six x-ray detectors are shown.

viewing angle is rotated to Doppler shift the photon energy ω_{lab} above the argon $L_{2,3}$ photoabsorption edge at $\omega_{\text{edge}} \approx 250$ eV. For $\beta=0.42$ this occurs at $\theta_{\text{lab}} \sim 95^\circ$.

The Doppler-tuned spectrometer uses six position-sensitive x-ray detectors. The detectors are multiwire, gas-filled proportional counters (position resolution ≈ 0.2 cm FWHM), arranged in a hexagonal ring around the ion beam with a beam-detector spacing of 72 cm. In front of each detector is a tapered Soller-slit collimator and a low-pressure argon-gas cell with thin polypropylene entrance and exit windows. The collimators are focused on a 1.2-cm-long section of the beam centered 1.3 cm downstream from the target where the $2^2P_{1/2}$ excited state is formed. The collimators are tapered so that each element of the x-ray detector views the same segment of beam from a slightly different angle, transforming the position response of the detector into an angular response. The entire spectrometer is enclosed in a 1.8-m-diam vacuum vessel maintained at a pressure of less than 5×10^{-4} Torr.

To determine the energy ω_{ion} of the x ray in the rest frame of the lithiumlike uranium ion we need three quantities: (a) the measured angle θ_{lab} between the beam and the photon detector at which an increase in photoabsorption occurs, (b) the measured beam velocity $\beta=v/c$, and (c) the energy $\omega_{\text{lab}}=\omega_{\text{edge}}$ of the argon $L_{2,3}$ edge. Rather than use the actual L edge, we enhance our resolution by using the nearby 244.39(0.01)-eV $2p-4s$ resonance transition.⁵ This resonance is well separated from the rest of the $L_{2,3}$ -edge structure (Fig. 2).

We measure θ_{lab} as follows: The position response of each detector is mapped by viewing 284-eV carbon K x rays from a stationary source through a mask inserted in front of the detector. The angle between the plane of the mask at its center and the nominal uranium beam axis is measured to ± 0.6 mrad using a front surface mirror mounted on a two-axis goniometer. This is done by aligning a telescope to the beam axis and then sighting on the mirror which we rotate to bring the center of the mask into view. The axis of the beam line is defined by the center wires of two removable position-sensitive particle detectors located 1.7 m upstream and 0.6 m downstream of the region viewed by the detectors. The uranium beam is then aligned through the centers of these particle detectors. The mechanical alignment is very stable and its measurement reproducible. We found no changes in the alignment over time and we found no changes in the alignment after a brief horizontal ground acceleration, estimated⁶ to be 0.1g, caused by the 1989 Loma Prieta earthquake.

The U^{89+} beam velocity is measured by time of flight (TOF) over a straight 1925.3(0.6)-cm path. The start and stop signals come from scintillator-photomultiplier detectors. The upstream scintillator and light seals are thin (0.0044 and 0.0030 cm, respectively) and their energy loss is separately measured and corrected for. Cable

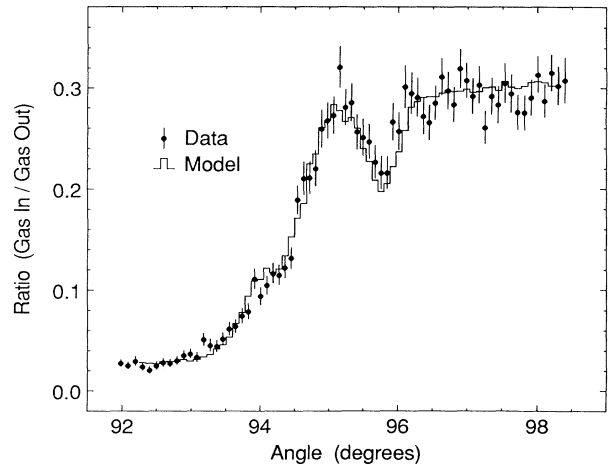


FIG. 2. Data for one run (of six) with one detector. The data points show the ratio of detected photon counts with argon gas in the cell to photon counts with no gas in the cell, plotted as a function of angle. In each case the counts are normalized to beam current. The uncertainties are statistical errors and the solid line is a fit of the Monte Carlo calculation to the data. The data shown here consist of 2.1×10^4 photon counts with gas in the cell, accumulated from an integrated beam on our target of 1.0×10^{10} U^{89+} ions plus 3.8×10^4 counts without gas, accumulated from 3.5×10^9 ions. During this run the average beam on our target was 2×10^6 ions per 1-s beam spill, with a repetition rate of 15 pulses/min.

and electronic delays are determined from TOF measurements over a short (30.8-cm) path.

In collecting data, we divide out any position-dependent detection efficiency by measuring the transmitted x-ray yield with, and without, argon gas in the gas cells. This is shown for one detector in Fig. 2, where the $L_{2,3}$ photoabsorption edge of argon is apparent as a step in the histogram at $\theta_{\text{lab}}=94.5^\circ$ and the $2p-4s$ resonance is seen at $\theta_{\text{lab}}=95.5^\circ$. Data are collected at two beam velocities, $\beta=0.423$ and 0.414. In Fig. 2 the beam velocity is $\beta=0.423$. At $\beta=0.414$ the spectra shift is about 0.8° , in agreement with Eq. (12) for $\omega_{\text{ion}} \approx 281$ eV. We observe the photoabsorption edge signals using gold and copper targets and different thicknesses of aluminum targets, confirming that the signal does not originate in the target atoms. The shape of the $L_{2,3}$ absorption edge is also observed to vary with argon-gas pressure, as expected. We measured the intensity of the photons as a function of the distance downstream from the target. The signal is observed to be an exponential decay over more than three mean lives (Fig. 3) with a lifetime of $61.8 \pm 1.2(\text{stat}) \pm 1.3(\text{syst})$ ps. This is in excellent agreement with the theoretical value of 60.7 ps for the $2^2P_{1/2}$ state lifetime obtained from Cheng, Kim, and Desclaux,⁷ corrected for our measured $2^2P_{1/2}-2^2S_{1/2}$ transition energy. The relativistic correction to the one-electron electric dipole ($E1$) matrix element⁸ decreases the decay rate by 37.3%. Our result is the most sensitive

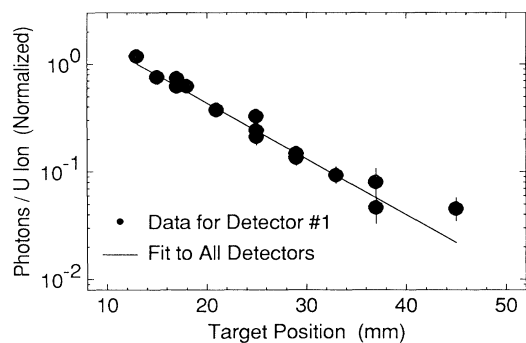


FIG. 3. Decay curve for $2^2P_{1/2} \rightarrow 2^2S_{1/2}$ in lithiumlike uranium.

test of the relativistic correction to the one-electron $E1$ matrix element.⁹

To find the center of the resonance dip we compare the observed spectra (Fig. 2) with a Monte Carlo calculation to account for, among other things, the angular resolution of the Doppler-tuned spectrometer, the finite decay length of the $2^2P_{1/2}$ state, the finite size, angular divergence, and energy spread of the beam, and the detailed structure of the argon absorption spectrum. The result of the Monte Carlo calculation for one detector is also shown in Fig. 2. Our result for six runs (divided between two beam velocities), each with six detectors, is 280.59(0.10) eV. The major sources of experimental uncertainty are shown in Table I.

Systematic error could arise from observing the transitions from other charge states present in the beam. The berylliumlike and heliumlike uranium ions produced in the target have $2p_{1/2} \rightarrow 2s$ transitions that are the analog of the lithiumlike $2^2P_{1/2} \rightarrow 2^2S_{1/2}$ transition. These transitions occur at approximately 295 eV in berylliumlike uranium⁷ and at 256 eV in heliumlike uranium,³ far outside the ≈ 1 eV instrumental resolution of our spectrometer. Other nearby transitions in the low-lying states of heliumlike, berylliumlike, and boronlike uranium arise from short-lived states that decay before reaching the measurement region.

Of particular concern is having the $1s^2p_{1/2} \rightarrow 1s^2s$ transition energy perturbed by a fourth "spectator" electron in a state of high principal quantum number (n). This system can be formed in the target, from ground-state lithiumlike uranium, when, in addition to a $2s \rightarrow 2p_{1/2}$ excitation, a fourth electron is captured into a high- n state. However, because of the ≈ 35 ps transit time of the beam between the target and the beginning of the measurement region, almost all of the high- n states decay to the $2s$ state before reaching the measurement region. For $n \geq 15$ some decay times are no longer sufficiently rapid, but, due to the high n , the population of these states is small, as is the perturbation of the spectator electron on the transition energy.

We estimate, using the equations in Ref. 10, that 20%

TABLE I. Sources of experimental uncertainty (68% confidence). The second column shows the size of the uncertainty per run and the third column the effect on the entire measurement.

| Source | Amount | Uncertainty in $h\omega$ (eV) |
|----------------------|-------------|-------------------------------|
| Beam velocity | 0.1% | 0.05 |
| Detector angle | 0.6 mrad | 0.05 |
| Fit to data | 0.3 channel | 0.05 |
| Detector calibration | 0.3 channel | 0.03 |
| Resonance energy | 0.03 eV | 0.03 |
| Total | | 0.1 |

of the lithiumlike uranium going through the target captures an electron, and about 11% of these are into states of $n > 15$. Thus a maximum of 2.2% of the signal can be generated from ions with four electrons.

To estimate the effect of the fourth electron on the $1s^2p_{1/2} \rightarrow 1s^2s$ transition energy we use both relativistic¹¹ and nonrelativistic¹² codes. They show that the effect decreases rapidly, with both increasing n and increasing angular momentum l . For a given n , the effect is largest if the fourth electron is in an s state. The low-lying s states, however, decay before reaching the measurement region. The lowest-lying s state with a lifetime greater than 1 ps is at about $n = 25$. The effect of a $25s$ electron is to increase the $1s^2p_{1/2} \rightarrow 1s^2s$ transition energy by only 0.01 eV. The corresponding p and d states decay faster than the s states and produce smaller effects. For the at most 2.3% of the atoms which reach the measurement region with a fourth electron in a high n, l state ($n > 15, l > 3$), the effect of the fourth electron is to increase the transition energy by less than 0.01 eV. A shift of 0.01 eV in 2.2% of the detected photons is insignificant.

We compare our experimental result of 280.59(0.10) eV with several recent calculations of the $2^2P_{1/2} \rightarrow 2^2S_{1/2}$ transition energy. A value of 281.02 eV has been obtained by Blundell, Johnson, and Sapirstein¹³ using a relativistic many-body perturbation theory (RMBPT) calculation of the non-QED contribution, and a value of 281.6 eV has been obtained by Indelicato and Desclaux¹⁴ using a multiconfiguration Dirac-Fock calculation. Both results include the authors estimates of the QED screening corrections and a separate estimate of the nuclear polarizability contribution.¹⁵ A separate calculation of the screening corrections to the self-energy (2.5 eV) and vacuum polarization (-0.6 eV) have been performed by Indelicato and Mohr¹⁶ and by Mohr,¹⁷ respectively. Combining the screening calculations with the one-electron QED (Ref. 18) (-42.8 eV) and the RMBPT calculation¹³ yields a value of 281.5 eV. Theoretical uncertainty of the order of 1 eV arises, predominantly in the parts of the calculations explicitly

involving more than one electron, from approximations and from uncalculated terms. By virtue of this large theoretical uncertainty, all of these calculations agree with our experiment.

To compare experiment with one-electron QED theory, we subtract from our experimental value the non-QED contribution of 322.4 eV from the RMBPT calculation (which includes the gross finite nuclear size effect) and the QED screening corrections of 1.9 eV. This yields $-43.7 \pm 0.10(\text{expt}) \pm \approx 1(\text{theory})$ eV compared to the calculated value of -42.8 eV. When the theoretical uncertainty has been reduced this result will improve significantly.

We thank Richard Claytor, Dennis Johnson, and Charles Munger for showing us how to improve our experiment; David Anderson, John Brown, and Ming Hui of LBL, and the instrument makers of the North Carolina State University College of Physical and Mathematical Sciences for assistance in spectrometer design, fabrication and assembly; Richard Leres for data-acquisition software, Margaret McMahan for electronics assistance, Norman Edelstein and Marcel Klapisch for running atomic structure codes, and the LBL Mechanical Technology Shop for building and assembling the detectors, to specification, budget, and deadline. We especially thank the operators and staff of the LBL SuperHILAC and Bevalac, who provided record extracted uranium beams of $> 10^7/\text{pulse}$. Except for one of us (L.L.), this work was supported by the Director, Office of Energy Research, Office of Basic Energy Sciences, Chemical Sciences Division, of the U.S. Department of Energy (DOE) under Contract No. DE-AC-02-76SF00098. One of us (B.F.) was supported by the Nuclear Physics Division of the U.S. DOE. One of us (L.B.) was supported by Ministère des Affaires Étrangères call bourse Lavoisier and the International Federation of University Women.

^(a)Present address: Quantum Metrology Division, National Institute of Standards and Technology, Gaithersburg, MD 20899.

^(b)Electronic address: belkacem@lbl.gov.

^(c)Permanent address: Section de Physique et Chimie, Institut Curie, 11 Rue Pierre et Marie Curie, 75005 Paris, France.

^(d)Present address: Department of Physics, University of

Pennsylvania, 209 S 33rd Street, Philadelphia, PA 19104.

^(e)Electronic address: feinberg@lbl.gov.

^(f)Electronic address: gould@lbl.gov.

^(g)Present address: Department of Physics, University of California, Berkeley, CA 94720.

^(h)Permanent address: 541 Woodmont Avenue, Berkeley, CA 94708.

⁽ⁱ⁾Permanent address: Department of Physics, North Carolina State University, Raleigh, NC 27695-8202.

^(j)Electronic address: kamphy@lbl.gov.

¹G. W. Erickson, *Phys. Rev. Lett.* **27**, 780 (1971); P. J. Mohr, *Ann. Phys. (N.Y.)* **88**, 26 (1974).

²For a review of strong field QED, see S. J. Brodsky and P. J. Mohr, in *Structure and Collisions of Ions and Atoms*, edited by I. A. Sellin, Topics in Current Physics Vol. 5 (Springer, Berlin, 1978), p. 3.

³C. T. Munger and H. Gould, *Phys. Rev. Lett.* **57**, 2927 (1986).

⁴R. W. Schmieder and R. Marrus, *Nucl. Instrum. Methods* **110**, 459 (1973); R. W. Schmieder, *Rev. Sci. Instrum.* **45**, 687 (1974); J. R. Huddle and J. R. Mowat, *Nucl. Instrum. Methods* **202**, 343 (1982).

⁵G. C. King *et al.*, *J. Phys. B.* **10**, 2479 (1977); M. Nakamura *et al.*, *Phys. Rev. Lett.* **21**, 1303 (1968); R. D. Deslattes, *Phys. Rev.* **186**, 1 (1969).

⁶B. Bolt, *Science* **251**, 133 (1991).

⁷K. T. Cheng, Y.-K. Kim, and J. P. Desclaux, *At. Data Nucl. Data Tables* **24**, 111 (1979).

⁸M. Hillery and P. J. Mohr, *Phys. Rev. A* **21**, 24 (1980).

⁹For an account of an earlier measurement, see R. Marrus, V. San Vicente, P. Charles, J. P. Briand, F. Bosch, D. Liesen, and I. Varga, *Phys. Rev. Lett.* **56**, 1683 (1986).

¹⁰W. E. Meyerhof *et al.*, *Phys. Rev. A* **32**, 3291 (1985).

¹¹M. Klapisch, A. Barshalom, and W. H. Goldstein, HULLAC code (unpublished); see also M. Klapisch, J. L. Schwob, B. S. Fraenkel, and J. Oreg, *J. Opt. Soc. Am.* **67**, 148 (1977).

¹²R. D. Cowan, *Phys. Rev.* **163**, 54 (1967); R. D. Cowan and D. C. Griffin, *J. Opt. Soc. Am.* **66**, 1010 (1976).

¹³S. A. Blundell, W. R. Johnson, and J. Sapirstein, *Phys. Rev. A* **41**, 1698 (1990).

¹⁴P. Indelicato and J. P. Desclaux, *Phys. Rev. A* **42**, 5139 (1990).

¹⁵G. Plunien, B. Müller, W. Greiner, and G. Soff, *Phys. Rev. A* **39**, 5428 (1989).

¹⁶P. Indelicato, and P. J. Mohr, in Proceedings of the Twelfth International Conference on Atomic Physics, Ann Arbor, Michigan, 29 July–3 August 1990 (to be published); (private communication).

¹⁷P. J. Mohr (private communication).

¹⁸W. R. Johnson and G. Soff, *At. Data Nucl. Data Tables* **33**, 405 (1985).